IAI Journals.ASM.org

Perforin-2 Restricts Growth of *Chlamydia trachomatis* in Macrophages

K. A. Fields, R. McCormack, L. R. de Armas, E. R. Podack

Department of Microbiology and Immunology, University of Miami Miller School of Medicine, Miami, Florida, USA

***Chlamydia trachomatis* is a Gram-negative obligate intracellular bacterium that preferentially infects epithelial cells. Professional phagocytes provide *C. trachomatis* only a limited ability to survive and are proficient killers of chlamydiae. We present evidence herein that identifies a novel host defense protein, perforin-2, that plays a significant role in the eradication of *C. trachomatis* during the infection of macrophages. Knockdown of perforin-2 in macrophages did not alter the invasion of host cells but did result in chlamydial growth that closely mirrored that detected in HeLa cells. *C trachomatis* L2, serovar B, and serovar D and *C. muridarum* were all equally susceptible to perforin-2-mediated killing. Interestingly, induction of perforin-2 expression in epithelial cells is blocked during productive chlamydial growth, thereby protecting chlamydiae from bactericidal attack. Ectopic expression of perforin-2 in HeLa cells, however, does result in killing. Overall, our data implicate a new innate resistance protein in the control of chlamydial infection and may help explain why the macrophage environment is hostile to chlamydial growth.**

Chlamydia trachomatis is a prevalent human pathogen responsible for sexually transmitted disease (serovars D to K and LGV1 to -3) and blinding trachoma (serovars A to C). The murine pathogen *C. muridarum* has been used historically to model human disease because the host immune response of mice to genital infections closely resembles that seen in humans (1). All *Chlamydia* spp. are obligate intracellular parasites that exhibit a biphasic developmental cycle (2). Infectious elementary bodies (EBs) initiate infection and differentiate into vegetative, but noninfectious, reticulate bodies (RBs). An unknown signal triggers the asynchronous conversion of RBs back into EBs, and the developmental cycle is completed by release from infected cells (3). Chlamydiae preferentially replicate in columnar epithelial cells (4) of respective mucosae, and development occurs entirely within a parasitophorous vacuole termed an inclusion. Inclusions convey a protected replication niche that remains segregated from the endosomal pathway and insulates intracellular chlamydiae from host defense and surveillance mechanisms (5). The privileged niche is created and maintained largely because of the deployment of potent antihost proteins (6, 7) via multiple secretory pathways (8).

Based on studies using *C. trachomatis* or *C. muridarum*, polymorphic neutrophils and macrophages are recruited to sites of infection *in vivo* (9) and the magnitude of this response correlates with ensuing immunopathologies indicative of *Chlamydia*-mediated disease (10). Although these chlamydial species are capable of infecting professional phagocytes such as monocytes and macrophages *in vitro* (11), growth is severely limited compared to that observed in epithelial cells. *C. trachomatis* infection of macrophages yields only 2 to 3% of the progeny detected in comparative epithelial infections. A majority of chlamydiae are rapidly targeted to Rab7-positive lysosomal compartments and do not incorporate viability biomarkers (12). Macrophage-dependent destruction of *C. trachomatis* has been associated with host cell autophagy (12–14), and treatment of macrophages with autophagy-inhibiting drugs such as bafilomycin A1 results in a modest increase in chlamydial growth (13, 14). Furthermore, autophagy-dependent killing of chlamydiae is enhanced after treatment with gamma interferon (IFN-γ) and requires the IFN-γ-inducible guanylate binding proteins (14). These observations emphasize the bactericidal capability of professional phagocytes toward *C. trachomatis* and imply a role for these cells in limiting chlamydial growth during a typical immune response.

Perforin-2 is encoded by macrophage-expressed gene 1 (15) and is constitutively expressed in macrophages. Mammalian perforin-2 is a ca. 74-kDa type I membrane protein with orthologues present in organisms as divergent as metazoans (16). Most significantly, perforin-2 contains a consensus membrane attack complex/perforin (MACPF) domain similar to those found in the membrane attack complex of complement and perforin-1. These domains are essential for protein polymerization and membrane insertion to form pores in bacterial cell walls or bilayer membranes. Expression of perforin-2 in macrophages, coupled with the similarity to perforin-1, has led to hypotheses suggesting an antibacterial function for perforin-2. Indeed, Wiens et al. linked perforin-2 to the innate defense against bacteria in the sponge *Suberites domuncula* (16). Most recently, the antibacterial activity of perforin-2 was directly demonstrated. Perforin-2 was essential for limiting the intracellular growth of *Salmonella enterica* serovar Typhimurium, *Mycobacterium smegmatis*, and *Staphylococcus aureus* in murine embryonic fibroblasts (17).

Multiple reports have documented the ability of professional phagocytes to directly kill intracellular chlamydiae (12, 14, 18). Given the constitutive expression of Mpeg1/perforin-2 in macrophages (15) and the role of perforin-2 in limiting intracellular bacterial replication (17), we questioned whether perforin-2 might contribute to the limitation of chlamydial growth in macrophages. We show herein that perforin-2 does restrict chlamydial

Received 20 April 2013 **Returned for modification** 10 May 2013
Accepted 3 June 2013
Published ahead of print 10 June 2013
Editor: R. P. Morrison
Address correspondence to K. A. Fields, Kfields@med.miami.edu.
Supplemental material for this article may be found at http://dx.doi.org/10.1128/IAI.00497-13.

doi:10.1128/IAI.00497-13

growth in macrophages. In addition, *Chlamydia* infection does not induce, and can actively repress, perforin-2 expression in HeLa cells. Chlamydiae, however, are susceptible to killing by ectopically expressed perforin-2. In aggregate, our data identify a novel host defense against chlamydial infection.

MATERIALS AND METHODS

Cell culture and organisms. These studies employed human HeLa 229 (CCL 21; American Type Culture Collection [ATCC], Manassas, VA) or A2EN primary-cell-like cervical epithelial cells (kindly provided by A. Quayle, Louisiana State University, Baton Rouge, LA). The macrophage-like lines used included murine BV2 (kindly provided by J. Bethea, University of Miami, Miami, FL) and RAW 264 (CRL-2278; ATCC). Eukaryotic cell lines were routinely maintained at 37°C in the presence of 5% CO_2–95% humidified air in RPMI 1640 medium (Invitrogen, Carlsbad, CA) supplemented with 10% (vol/vol) fetal bovine serum (Sigma-Aldrich, St. Louis, MO). A2EN cells were grown as nonpolarized monolayers in EpiLife serum-free medium supplemented with Define Growth Supplement (Life Technologies, Grand Island, NY). These studies employed *C. muridarum* (strain Nigg) and *C. trachomatis* LGV-434 (serotype L2), TW-5/OT (serotype B), and UW-3/CX (serotype D). Density gradient-purified EBs were purified, stored as described previously (19), and used for infections. Heat-killed (HK) chlamydiae were prepared by the treatment of equivalent numbers of EBs for 30 min at 80°C. Primary infections were carried out in Hanks' balanced salt solution (HBSS; Invitrogen) for 1 h at 37°C. Infected cells were washed and incubated for different times at 37°C in the presence of 5% CO_2–95% humidified air. Where indicated, cultures were supplemented with 10 U/ml IFN-γ (PeproTech, Rocky Hill, NJ) or 200 μg/ml chloramphenicol (Sigma, St. Louis, MO). Where appropriate, primary cultures were lysed in ice-cold sucrose-phosphate-glutamate buffer (SPG; 10 mM sodium phosphate, 8 mM Na_2HPO_4–2 mM NaH_2PO_4, 220 mM sucrose, 0.50 mM L-glutamic acid) at the indicated times, diluted in SPG, and replated on fresh HeLa cells for enumeration of progeny inclusion-forming units (IFUs) as described previously (20).

Immunoblot analysis. Respective cultures were processed for immunoblot analysis via lysis in ice-cold water supplemented with protease inhibitor cocktail (EMD Millipore). Cultures were pretreated with MG-132 as described previously (17) for 30 min prior to harvesting for experiments assessing perforin-2 levels in HeLa cells. Proteins were precipitated from lysates by the addition of trichloroacetic acid (Sigma) to 10% (vol/vol). Concentrated material was solubilized in Laemmli electrophoresis sample buffer (21), resolved in polyacrylamide gels, and subsequently transferred to Immobilon-P (Millipore, Corp., Bedford, MA). Specific proteins were detected by probing with anti-murine or anti-human Mpeg1 (Abcam, Cambridge, MA), anti-indoleamine 2,3-dioxygenase (IDO; EMD Millipore), or anti-β-actin (Sigma) antibody, followed by appropriate horseradish peroxidase-conjugated secondary antibodies (Sigma). Visualization was achieved by development with ECL Plus chemiluminescent substrate (GE Healthcare, Buckinghamshire, United Kingdom). Densitometry analysis of immunoblot assay signals was accomplished with an AlphaImager and associated image analysis software (Alpha Innotech, Corp., San Leandro, CA).

Fluorescence microscopy. Microscopy was employed to assess protein localization in infected and transfected host cells. BV2 or HeLa cell monolayers were grown as described previously (22) on 12-mm-diameter coverslips. For transfection studies, HeLa cells were transfected with red fluorescent protein (RFP) or RFP–perforin-2 by using Lipofectamine 2000. At the postinfection times indicated, monolayers were fixed and permeabilized with methanol; blocked with 5% (wt/vol) bovine serum albumin and 0.1% (vol/vol) mouse serum in phosphate-buffered saline supplemented with 0.05% (vol/vol) Tween 20 (Sigma); and probed with *Chlamydia*-specific antibodies. Proteins were visualized by probing with Alexa 488-conjugated goat anti-rabbit antibodies (Invitrogen). Epifluorescence images were acquired on a TE2000U inverted photomicroscope (Nikon Inc., Melville, NY) equipped with a Retiga EXi 1394 12-bit monochrome charge-coupled device camera (QImaging, Surrey, BC, Canada) and MetaMorph imaging software version 6.3r2 (Molecular Devices, Downingtown, PA). Where appropriate, inclusion areas were computed from acquired images by using the MetaMorph region measurement function.

Invasion assay. Quantitation of invasion efficiency was performed essentially as described previously (23). Briefly, host cells were cultivated on 12-mm glass coverslips in triplicate and infected for 1 h at 4°C with fluorescently 5(and 6)-{[(4-chloromethyl)benzoyl]amino}tetramethylrhodamine-labeled *C. trachomatis* L2 at an apparent multiplicity of infection (MOI) of 10. Unattached chlamydiae were washed away with HBSS containing 2 μg/ml heparin, and invasion was initiated by the addition of warm medium. Cultures were fixed with 4% paraformaldehyde after 20 min of incubation at 37°C. Nonpermeabilized samples were blocked and probed with *C. trachomatis* major outer membrane protein-specific antibodies, followed by Alexa 488-conjugated secondary antibodies to detect extracellular chlamydiae. Samples were processed for fluorescence microscopy, and 100 bacteria per treatment were assessed in triplicate as extracellular (green and red) or intracellular (red only).

Transmission electron microscopy (TEM). Cells were grown to semiconfluence on 13-mm glass coverslips and infected with *C. trachomatis* as described previously (24). Infected monolayers were incubated for 24 h at 37°C in RPMI and subsequently prepared by fixation in 4% (wt/vol) paraformaldehyde–2.5% (vol/vol) glutaraldehyde in 100 mM sodium cacodylate, pH 7.4. Samples were postfixed in 2% osmium tetroxide in 0.1 M phosphate buffer and dehydrated through graded ethanol solutions. Finally, material was embedded in EM-bed (Electron Microscopy Sciences, Fort Washington, PA), cut into 80-nm sections on a Leica Ultracut-R ultramicrotome, and negatively stained with uranyl acetate and lead citrate. The grids were viewed at 80 kV on a Philips CM-10 transmission electron microscope, and images were captured by a Gatan ES1000W digital camera.

Quantitation of gene expression via quantitative RT-PCR. Whole-culture RNA was extracted by using TRIzol reagent (Life Technologies) according to the manufacturer's instructions. Preparations were treated with RQ1 DNase (Promega, Madison, WI), and RNA was converted to cDNA with a QuantiTect reverse transcription (RT) kit (Qiagen, Valencia, CA). Murine (BV2) or human (HeLa and A2EN) Mpeg1 was amplified by RT-PCR as described previously (17), with Applied Biosystems TaqMan Gene Expression Assays (Life Technologies). Message for the glyceraldehyde 3-phosphate dehydrogenase (GAPDH)-encoding housekeeping gene was amplified as an internal normalization control. All assays were performed in triplicate for each RNA sample.

RNA interference. For murine cells, three Mpeg1-specific chemically synthesized 19-nucleotide small interfering RNA (siRNA) duplexes were obtained from Sigma. Two siRNAs were complementary to the 3′ untranslated region of perforin-2, and the third was complementary to the coding region. The sequences were CCACCUCACUUUCUAUCAA, GAGUAUUCUAGGAAACUUU, and CAAUCAAGCUCUUGUGCAC. Two scrambled siRNAs were also generated to serve as a control for the reaction. Transfection of siRNA into all cells was carried out with the Amaxa Nucleofector System (Lonza) according to the manufacturer's instructions. All transfections were carried out with 1×10^6 to 4×10^6 cells, a final concentration of 1 μM siRNA (perforin-2-specific siRNAs were pooled), and 2 μg of plasmid DNA where indicated. Immediately after transfection, cells were plated in antibiotic-free complete medium.

RESULTS

We began testing our hypothesis by employing siRNA-mediated knockdown of perforin-2 expression in BV2 macrophages. BV2 cells were transfected with perforin-2-specific or control siRNAs and subsequently infected with *C. trachomatis* L2. Examination of infected cultures 24 h postinfection revealed dramatic differences in chlamydial content (Fig. 1A). Material that reacted with *Chla-*

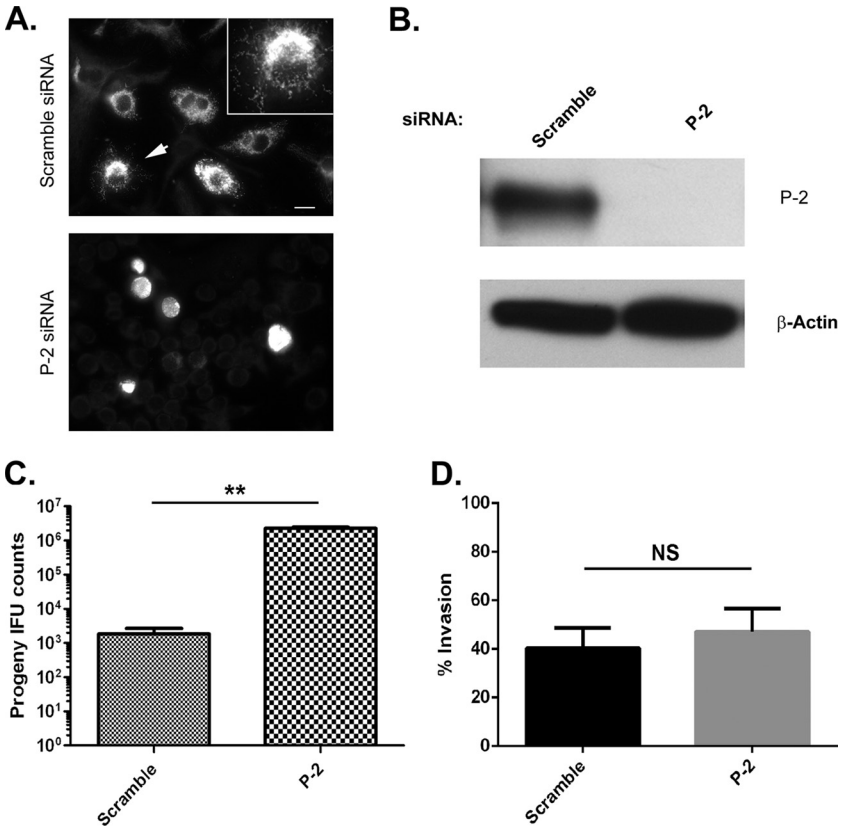

FIG 1 Perforin-2 inhibits intracellular proliferation of *C. trachomatis* in macrophages. BV2 cells were transfected with either perforin-2-specific siRNA or scrambled siRNA as a negative control. Cultures were infected with *C. trachomatis* L2 at an MOI of 0.5 roughly 24 h posttransfection and examined or harvested 24 h postinfection. (A) Cultures were processed for analysis via indirect immunofluorescence assay by probing with anti-*Chlamydia* antibodies. The arrow indicates the enlarged area in panel A. Bar = 5 μm. (B) Whole-culture material from scrambled-siRNA- or perforin-2 (P-2) siRNA-treated cells was probed via immunoblot assay with anti-perforin-2 or anti-β-actin antibody as a loading control. (C) Data for progeny counts are represented as means ± standard deviations of triplicate samples, and a Student *t* test was used to assess the statistical significance of differences (**; $P < 0.002$). (D) Data for invasion efficiency are presented as mean percentages of bacteria ($n = 100$ in triplicate cultures) internalized ± standard deviations. A Student *t* test indicated no significant difference (NS).

mydia-specific antibodies was routinely detected in dispersed, punctate patterns in control BV2 cells, whereas mature inclusions were rarely observed. This pattern is consistent with a previous report indicating killing of chlamydiae in macrophages via autophagy (12). In contrast, treatment of cells with perforin-2 siRNA resulted in the routine detection of apparently intact, mature chlamydial inclusions. Perforin-2 knockdown was efficient since immunoblot analysis of material harvested from parallel cultures revealed that perforin-2 levels were below the limit of detection in cells treated with perforin-2-specific siRNA (Fig. 1B). We next quantitatively assessed chlamydial growth by enumerating progeny EBs from cultures pretreated with scrambled or perforin-2-specific siRNA. Progeny EB numbers were elevated ca. 1,000-fold in cultures where perforin-2 was knocked down (Fig. 1C). This effect was not cell line specific since similar results were detected when RAW macrophages were used as host cells (see Fig. S1 in the supplemental material). Moreover, the increased progeny counts were not due to more efficient invasion of perforin-2 siRNA-treated cells. Direct quantitation of chlamydial invasion revealed no differences between control and perforin-2 knockdown cells (Fig. 1D). Collectively, these data indicate that perforin-2 is important for macrophage-mediated inhibition of intracellular *C. trachomatis* proliferation.

We considered the possibility that perforin-2 susceptibility could be *Chlamydia* species specific since *C. trachomatis* L2 is a human pathogen that is rapidly cleared in the murine infection model (25). In addition, knockdown of perforin-2 in BV2 cells appeared to result in robust chlamydial growth, raising the possibility that growth comparable to that detected in epithelial cells could be supported. Both of these possibilities were tested by infection of BV2 and HeLa cells with the same inocula of *Chlamydia*. In addition to *C. trachomatis* L2, we chose to test additional human pathogens of the ocular (serovar B) or genital (serovar D) serovar, as well as the murine pathogen *C. muridarum*. Consistent with our previous data obtained with *C. trachomatis* L2, detection of mature inclusions harboring the additional chlamydial strains was rare in BV2 cells transfected with scrambled siRNA. However, large inclusions were detected for all *Chlamydia* in the absence of perforin-2 (Fig. 2A). The results correlated with the quantitative enumeration of inclusions in primary cultures (Fig. 2B). Knockdown of perforin-2 resulted in inclusion numbers approaching those detected in HeLa cells for *C. trachomatis* L2 and *C. muridarum*. *C. trachomatis* serovar B and D inclusions were ca. 20% as numerous as those in parallel HeLa cell cultures. Measurement of inclusion areas (Fig. 2C) revealed that those inclusions that were detectable in control BV2 cells expressing perforin-2 were signif-

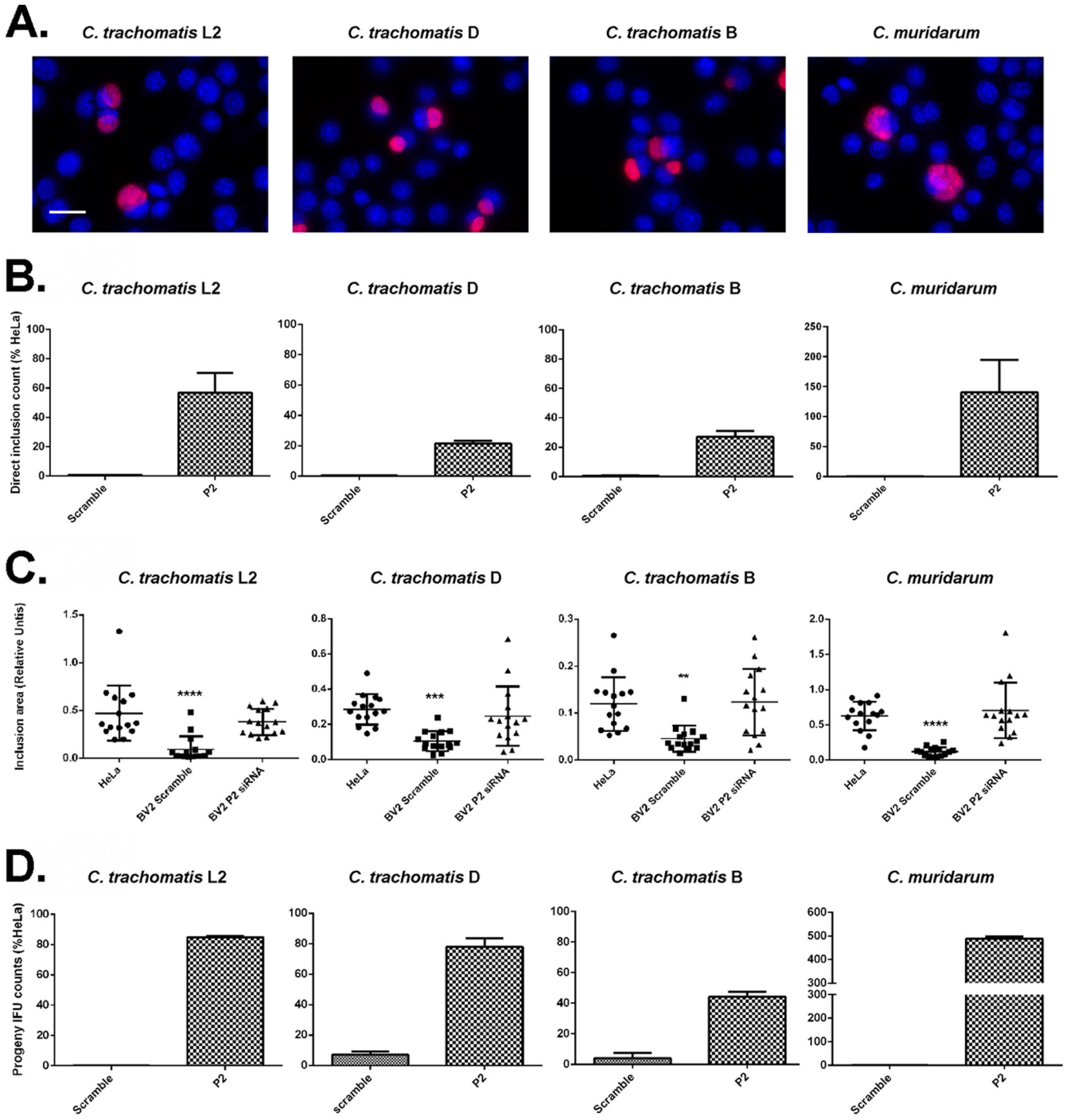

FIG 2 Perforin-2 inhibits the growth of multiple *Chlamydia* serovars and species. BV2 (treated with scrambled siRNA or perforin-2 siRNA) and HeLa cells were infected with the same inocula containing *C. muridarum* or *C. trachomatis* serovar L2, D, or B. Cultures were fixed and stained to visualize chlamydial inclusions via indirect immunofluorescence assay (A to C) or harvested for enumeration of progeny chlamydiae (D). (A) Representative immunofluorescence micrographs of *Chlamydia* inclusions (red) within BV2 cells treated with perforin-2-specific siRNA. Host cell nuclei are also shown (blue). Bar = 5 μm. (B) Inclusion counts during primary infections are reported as the percentages of mature inclusions detected in BV2 cells compared to those in equivalently infected HeLa cells. (C) Areas of representative inclusions were measured and plotted with respective means and standard deviations shown. One-way ANOVA was used to compute the statistical significance of area measurement differences from those of HeLa control cells (****, $P < 0.0001$; ***, $P < 0.0003$; **, $P < 0.0051$). (D) Progeny inclusion counts are reported as the percentages of mature inclusions detected in BV2 cells compared to those in equivalently infected HeLa cells.

icantly smaller than inclusions in HeLa cells. In contrast, inclusions in BV2 cells lacking perforin-2 were not significantly different in size from those detected in HeLa cells. Finally, we assessed growth by enumeration of progeny chlamydiae in BV2 cells compared to HeLa cells (Fig. 2D). In the presence of perforin-2 (scrambled-siRNA control), the progeny counts were less than 5% of those in HeLa cells for all of the *Chlamydia* strains tested. Depletion of perforin-2 resulted in progeny levels approaching those

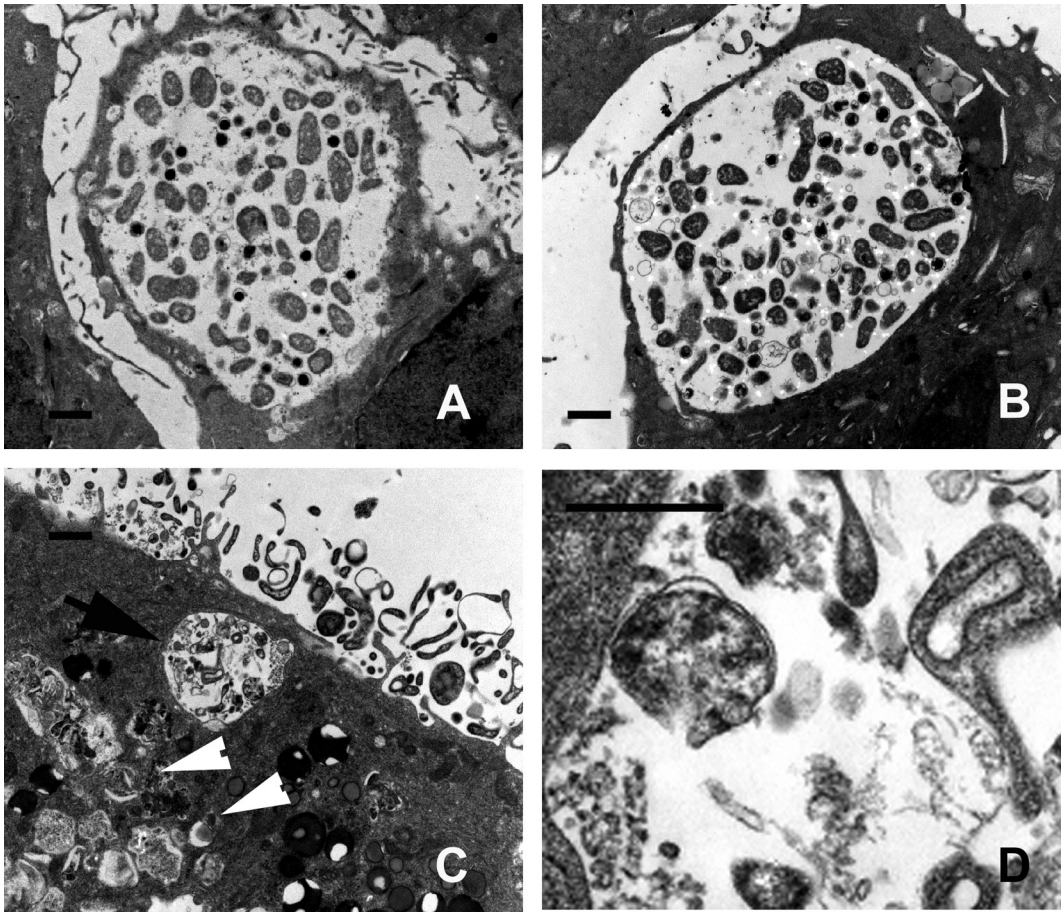

FIG 3 Electron microscopic evidence of intact inclusions in perforin-2 siRNA-treated cells. BV2 cells were transfected with scrambled siRNA or perforin-2-specific siRNA and infected 24 h later with *C. trachomatis* L2 at an MOI of 1. HeLa cells were also infected as a control. Cultures were processed for TEM analysis at 24 h postinfection. All images were acquired at a magnification of ×7,900, and representative micrographs are shown for HeLa cells (A) or BV2 cells lacking (B) or containing (C) perforin-2. (C) Arrows indicate typical *Chlamydia*-containing vacuoles detected in scrambled-siRNA-treated cells. The black arrow indicates the enlarged area shown in panel D.

detected in HeLa cells for all of the *C. trachomatis* serovars. Interestingly, the *C. muridarum* progeny counts were reproducibly in excess of those in HeLa cells. We conclude that knockdown of perforin-2 renders BV2 macrophages nearly as susceptible to *Chlamydia* infection as the permissive epithelial host cells are.

TEM was employed to examine the comparative fitness of inclusions in BV2 cells containing or lacking perforin-2. HeLa cells or siRNA-treated BV2 cells were infected with *C. trachomatis* L2 and processed for TEM at 24 h postinfection (Fig. 3). As expected, HeLa cells contained large inclusions that contained a mixture of RBs and smaller, electron-dense EBs. A similar pattern was seen in BV2 cells that were pretreated with perforin-2-specific siRNA. In contrast, scrambled-siRNA-treated control BV2 cells typically contained multiple small vacuoles that often seemed to contain a single bacterium. When larger vacuoles were detected, the lumen appeared congested with debris and RBs were deformed or lacked intact envelopes. These data are consistent with the comparatively limited capacity of chlamydiae to replicate within macrophages. In addition, they provide evidence that perforin-2 contributes to the inhibition of chlamydial growth in these professional phagocytes.

Although perforin-2 expression is constitutive in macrophages, the observation that its expression is inducible by exogenous agents (17) raised the possibility that chlamydial infection might further increase perforin-2 levels in macrophages. This possibility was tested by assessing perforin-2 message and proteins levels during a chlamydial infection (Fig. 4). BV2 cells were mock infected or infected with *C. trachomatis* L2, and whole-culture protein or RNA was harvested over time from parallel cultures. Protein and mRNA abundances were subsequently determined by immunoblot assay of concentrated proteins or quantitative PCR of cDNA, respectively. Consistent with constitutive production, perforin-2 was detected at all of the time points tested (Fig. 4A). Perforin-2 protein abundance remained unaltered through 6 h postinfection, whereas a noticeable increase in perforin-2 levels was apparent at 12 and 24 h. Perforin-2 mRNA levels revealed a similar pattern. *Chlamydia* infection resulted in a statistically significant increase in perforin-2 message as early as 6 h postinfection (Fig. 4B). Abundance continued to increase and was induced ca. 16-fold relative to that in the mock-treated control by 24 h postinfection. These data indicate that chlamydial infection of BV2 macrophages induces the expression of perforin-2.

Collectively, our data clearly implicate perforin-2 in the macrophage-dependent control of chlamydial growth. Interestingly,

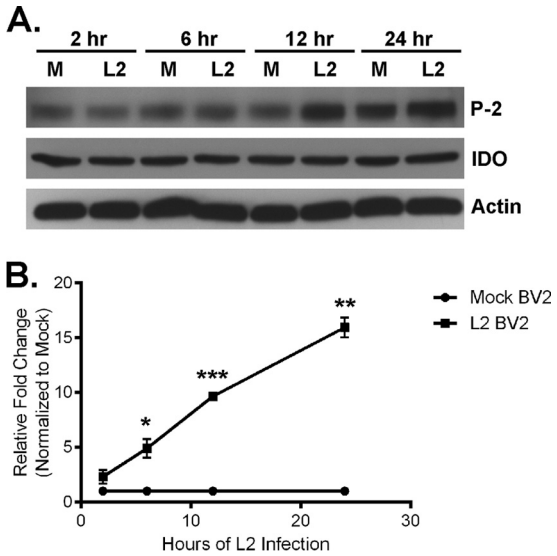

FIG 4 *Chlamydia* infection induces perforin-2 expression in macrophages. Parallel BV2 cultures were mock infected (M) or infected with *C. trachomatis* (L2) at an MOI of 1, and whole-culture protein (A) or RNA (B) was harvested at 2, 6, 12, and 24 h postinfection. (A) Endogenous perforin-2 was detected in immunoblot assays with perforin-2-specific antibodies, and IDO and β-actin were visualized as controls. (B) Message levels were evaluated by quantitative PCR of cDNA. The perforin-2 message level was normalized to the GAPDH signal, and *n*-fold change is relative to a mock-treated control. Student's *t* test was used to evaluate the statistical significance of differences at each time point between triplicate mock- and *Chlamydia*-infected samples (*, $P < 0.01$; **, $P < 0.001$; ***, $P < 0.0001$).

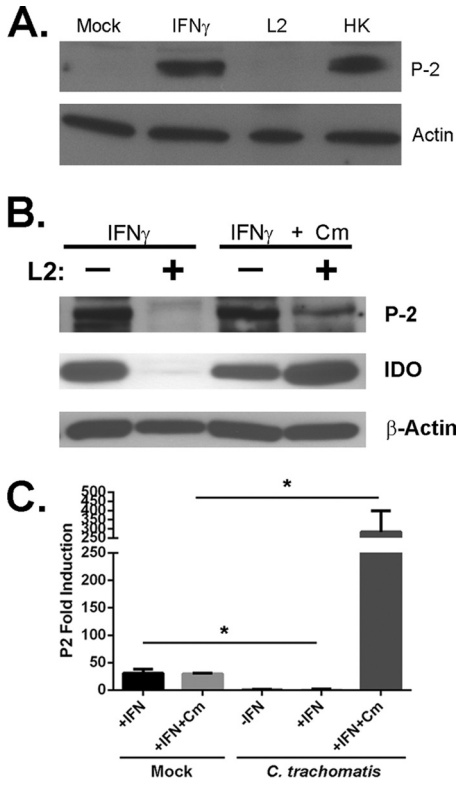

FIG 5 Perforin-2 expression in *C. trachomatis*-infected HeLa cells. (A) HeLa cells were mock treated, infected with *C. trachomatis* (L2) for 24 h, or treated with 10 U/ml IFN-γ or HK chlamydiae for 15 h. Immunoblot assays of whole-culture material were probed with antibodies specific for endogenous perforin-2 (P-2) or β-actin as a loading control. (B) HeLa cells were mock infected or infected at an MOI of 1 with *C. trachomatis* L2. Cultures were supplemented with 10 U/ml IFN-γ with or without 200 μg/ml chloramphenicol (Cm) at 24 h postinfection. Whole-culture protein was harvested 15 h later. Endogenous perforin-2 was detected in immunoblot assays, and IDO and β-actin were visualized as controls. (C) Quantitative PCR of cDNA was done to determine message levels in cultures treated as described for panel B. The perforin-2 (P2) message level was normalized to the parallel GAPDH signal, and *n*-fold change is compared to the appropriate mock-infected control. Data are presented as means ± standard deviations of triplicate samples (*, $P < 0.01$).

many cell types, including epithelial cells, are capable of expressing perforin-2 (R. McCormack et al., unpublished data). This observation raises the question of whether chlamydiae need to contend with perforin-2 in epithelial cells. Perforin-2 levels were evaluated in HeLa cells that were either mock treated or infected with viable or HK *C. trachomatis* (Fig. 5A). Treatment of cells with exogenous IFN-γ was used as a positive control for perforin-2 induction. Perforin-2 was not detected in mock-treated samples or cells infected with viable chlamydiae. This pattern was also seen when culture lysates were generated in the presence of 8 M urea to prevent the previously reported (26) possibility of postlysis degradation of host proteins (data not shown). In contrast, perforin-2 was apparent in cells treated with IFN-γ or HK chlamydiae. Therefore, perforin-2 expression is not constitutive in HeLa cells but is inducible by appropriate stimuli. Further, chlamydiae obviously contain products capable of stimulating perforin-2 production since perforin-2 was detected in cells treated with HK chlamydiae. Since perforin-2 was below the level of detection in the presence of viable *Chlamydia*, this raised the possibility that active infection by live chlamydiae suppresses or avoids pathways involved in the induction of perforin-2 expression.

We examined whether *Chlamydia* infection of epithelial cells actively suppresses perforin-2-inducing pathways by combining infection and IFN-γ stimulation (Fig. 5B). HeLa cells were infected with *C. trachomatis* for 24 h, and IFN-γ was included during the last 15 h. In addition, parallel cultures were also treated with chloramphenicol for the last 15 h to block chlamydial *de novo* protein synthesis. We harvested whole-culture protein for assessment of perforin-2 levels. Immunoblots were probed with perforin-2 antibodies or antibodies specific for IDO or β-actin as controls (Fig. 5B). As expected, perforin-2 was detected in uninfected HeLa cells that were treated with IFN-γ. However, similar IFN-γ treatment of *Chlamydia*-infected HeLa cells did not result in detectable perforin-2. A similar pattern was seen for IDO. The magnitude of the *Chlamydia*-dependent decrease in the abundance of perforin-2 and IDO was reduced in cultures treated with chloramphenicol. We next extended our analysis by testing levels of perforin-2-specific message via quantitative PCR of whole-culture cDNAs (Fig. 5C). As expected, expression was induced when uninfected cells were treated with IFN-γ. Consistent with immunoblot assay data, perforin-2 mRNA was significantly decreased when IFN-γ-treated cells contained viable chlamydiae. Interestingly, perforin-2 mRNA was induced an additional ca. 10-fold when infected cultures were treated with chloramphenicol. Perforin-2 mRNA was also examined during the infection of human primary-cell-like A2EN cells to exclude the possibility of cell line-specific effects (see Fig. S2 in the supplemental material). Similar to HeLa cells, A2EN perforin-2 mRNA was also induced by IFN-γ treatment and induction was inhibited in cultures infected with *C. trachomatis*. These observations were also not specific to the host

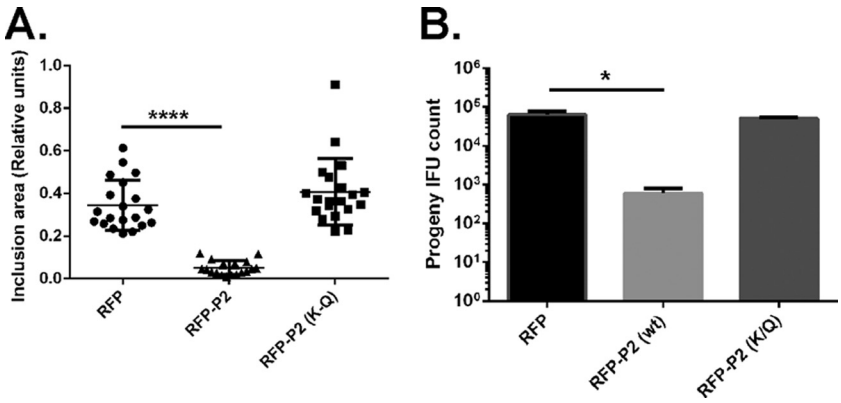

FIG 6 Ectopic expression of perforin-2 in HeLa cells suppresses chlamydial growth. HeLa cells were transfected with plasmids encoding RFP or RFP–perforin-2 and infected 6 h later with *C. trachomatis* L2. An inactive version of perforin-2 carrying a K→Q mutation [RFP-P2 (K/Q)] was included as an additional negative control. At 24 h postinfection, parallel cultures were fixed and stained and inclusion areas were calculated (A) or cells were harvested for progeny IFU counting (B). One-way ANOVA was used to compute the statistical significance of area measurement differences from the RFP control (****, $P < 0.0001$) or progeny count differences from the RFP control (*, $P < 0.01$). wt, wild type.

species since identical results were obtained with murine CMT93 epithelial cells (data not shown). In aggregate, the data indicate that established chlamydial infection can actively repress IFN-γ-mediated induction of perforin-2. This effect is manifested at the level of transcription and requires continued *de novo* protein synthesis by chlamydiae.

Given the observed inhibition of endogenous perforin-2 expression, ectopic expression from a constitutively active promoter was used to assess the susceptibility of chlamydiae to perforin-2 in epithelial cells (Fig. 6). HeLa cells were first transfected with perforin-2–RFP and then infected with *C. trachomatis* L2. Transfections with RFP only or perforin-2–RFP containing inactivating Lys-to-Glu mutations at residues 197, 199, and 200 of peforin-2 were used as negative controls. Chlamydial growth was assayed at 20 h postinfection by direct measurement of inclusion areas in transfected cells (Fig. 6A) or harvesting of whole cultures for subsequent enumeration of progeny EBs (Fig. 6B). A significant reduction in inclusion areas was detected when active perforin-2–RFP was present. Likewise, progeny counts were reduced ca. 100-fold. Hence, perforin-2 is capable of inhibiting chlamydial growth within epithelial cells.

Perforin-2 is a putative pore-forming protein capable of disrupting the integrity of bacterial envelopes (17). Perforin-2 could interfere with chlamydial viability by targeting the inclusion membrane and/or the bacteria directly. Immunolocalization was employed to examine whether perforin-2–RFP gains access to the *Chlamydia*-containing vacuole (Fig. 7). HeLa cells were transfected with RFP-containing constructs for either 24 or 6 h prior to infection with *C. trachomatis* L2. Infected cells were then paraformaldehyde fixed 20 h postinfection. Chlamydiae were visualized by probing with whole-*Chlamydia* antibodies. RFP-only signal was routinely detected throughout the host cytosol and did not appear to concentrate near the inclusion. In contrast, both perforin-2–RFP and an inactive version of perforin-2 carrying a K→Q mutation were often detected in a rim-like pattern surrounding the chlamydial inclusion when transfection was followed closely by infection. Although inclusions appeared intact in the presence of perforin-2–RFP, anti-*Chlamydia* antibody staining was consistent with disrupted bacteria since spherical bacteria were rarely observed. Interestingly, intact inclusions were not detectable

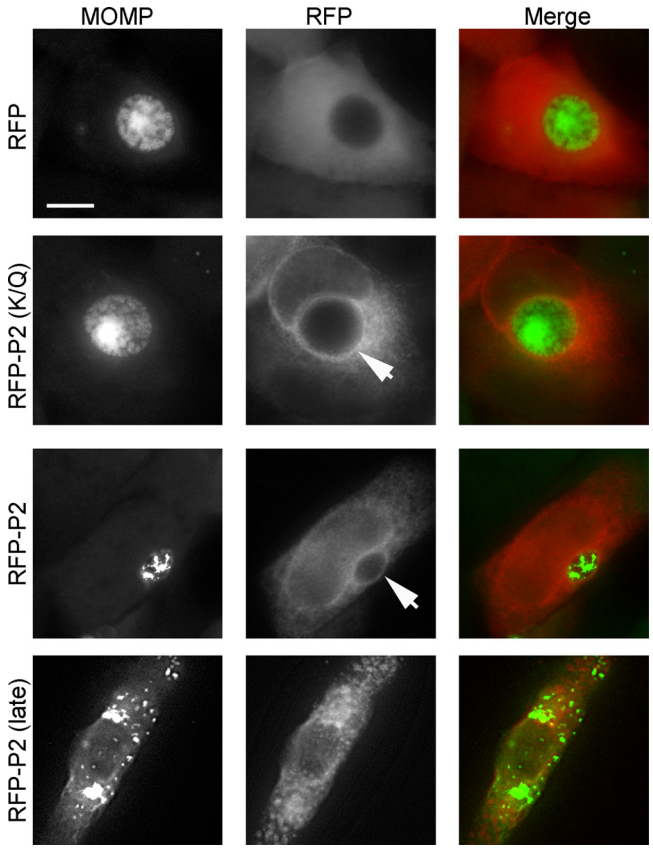

FIG 7 Perforin-2 localization during chlamydial infection. HeLa cells were transfected with RFP and an inactive version of perforin-2 carrying a K→Q mutation [RFP-P2 (K/Q)] 6 h prior to infection. Parallel cultures were also transfected with perforin-2–RFP (RFP-P2) 6 or 24 h (late) before infection. *C. trachomatis* L2 was used to infected cells at an MOI of 1, and cultures were fixed and stained with *Chlamydia*-specific antibodies at 24 h postinfection. RFP-containing proteins (red) are shown with chlamydiae (green), and the rim-like localization of perforin-2–RFP and perforin-2 (K/Q)–RFP is marked by arrows. Bar = 5 μm. MOMP, major outer membrane protein.

when perforin-2 was expressed 24 h prior to infection. Instead, material reactive with *Chlamydia*-specific antibodies was dispersed in a punctate pattern that often correlated with perforin-2–RFP-specific signals. Hence, perforin-2 gains access to chlamydiae, where it could inhibit growth by killing the bacteria.

DISCUSSION

Mpeg1 was originally discovered during the screening of cDNA to identify gene products associated with mature macrophages (15). Further analysis in that original study failed to detect Mpeg1 expression in other cell types. However, McCormack et al. (17) established that Mpeg1 expression is detectable in fibroblasts treated with type I or II IFN, raising the possibility of inducible expression in other cell types. Subsequent analysis of the deduced protein sequence revealed the presence of a MACPF domain. The function of this conserved domain is best described in perforin-1 (27) and the membrane attack complex complement component C9 (28, 29), where the domain is essential for the formation of membrane-spanning pores (30, 31). Complement targets bacterial envelopes, whereas perforin-1 mediates perforation of eukaryotic plasma membranes. Like complement, perforin-2 has been shown to limit bacterial growth (17). Perforin-2 is likely not a secreted protein since the deduced amino acid sequence contains a predicted transmembrane domain and RFP-tagged perforin-2 colocalizes with host perinuclear vesicles with perforin-2 embedded in the membrane. Therefore, it is most likely that perforin-2 exerts antimicrobial activity directed toward intracellular and/or cell-associated bacteria. Collectively, these data have led to a working model (17) whereby perforin-2 contributes to innate immunity via trafficking to, and direct disruption of, intracellular bacteria.

Our data are consistent with this model. Perforin-2 is clearly capable of interfering with chlamydial growth, and our microscopic analyses are consistent with disruption of the bacteria. In addition, development was not merely delayed, since experiments at later time points revealed greater decreases in infectious progeny (data not shown). Commercially available perforin-2-specific antibodies detect denatured perforin-2 but were ineffective at detecting endogenous native perforin-2 via indirect immunofluorescence assay (data not shown), yet RFP-tagged perforin-2 colocalized with chlamydial inclusions. At later time points, RFP–perforin-2 could also be detected in punctate foci that also contained anti-*Chlamydia*-reactive material. Hence, it is clear that perforin-2 eventually gains access to chlamydiae. Since chlamydial inclusions avoid fusion with vesicles of the endocytic pathway (5), it is likely that perforin-2 is delivered by an alternate mechanism. Indeed, perforin-2–RFP can be detected in host perinuclear membrane vesicles (McCormack et al., unpublished). The chlamydial inclusion interacts with the endoplasmic reticulum and the Golgi compartment to acquire lipids (reviewed in reference 32), and both of these organelles could be a source of perforin-2 vesicles. Hence, direct transfer of perforin-2 from these organelles to the inclusion could occur in cells that express the protein. Given the variety of bacteria that are susceptible to perforin-2-mediated killing (17), however, it is equally possible that a more generalized, pathogen-activated trafficking pathway enables perforin-2 to gain access to cell-associated bacteria. Since an intact inclusion is essential for chlamydial development, we could not differentiate whether perforin-2 antichlamydial activity was manifested at the inclusion membrane, the chlamydial envelope, or both. In accordance with the working model, we hypothesize that perforin-2 would form pores in the chlamydial outer membrane. Clearly, significant work is required to establish the precise molecular mechanisms that govern perforin-2 activity.

Although chlamydial infection of monocytes has been proposed for trafficking to distal sites of infection, the macrophage is clearly not a hospitable replicative niche for *C. trachomatis* (reviewed in reference 11). Survival in macrophages has been described as biovar dependent, with the LGV biovar exhibiting a resistance to killing greater than that of non-LGV *C. trachomatis* (33).

We observed that the absence of perforin-2 enabled significant chlamydial growth in macrophages that was independent of the chlamydial biovar and species. Indeed, knockdown of perforin-2 enabled levels of growth of *C. trachomatis* L2, B, and D and *C. muridarum* that approached or exceeded those seen in HeLa cells. Interestingly, elicited peritoneal macrophages express active perforin-2 (McCormack et al., unpublished), yet both *C. psittaci* (34) and *C. muridarum* (35) have been described as being able to productively grow in these primary murine macrophages. Indications are that *C. muridarum* growth is somewhat less efficient in these macrophages than in fibroblasts (35), raising the possibility of perforin-2-mediated killing. Since it is possible to achieve nearly 100% infection, however, we cannot exclude the possibility that *C. muridarum*-specific protective mechanisms are manifested in these cells that protect it from perforin-2-mediated killing.

Autophagy has also been shown to exert a role in limiting chlamydial infection in macrophages (12, 14) and could represent a synergistic mechanism to control the intracellular growth of chlamydiae. Inhibition of macrophage autophagy via bafilomycin A1 (12) or knockdown of ATG5 (14) was reported to result in a modest (<5-fold) increase in chlamydial infectivity. Our own observations are consistent with these reports (data not shown). In contrast, we observed increases in chlamydial infectivity that exceeded multiple logs. Therefore, we predict that perforin-2 functions upstream of autophagy and is not entirely dependent on the formation of a mature autophagosome.

Our data indicate that chlamydiae are protected from perforin-2-mediated killing in epithelial cells by prevention of perforin-2 expression at the transcriptional level. This is consistent with the epithelial cell representing the preferred intracellular replication niche and is in contrast to the observed induction of perforin-2 message in BV2 cells. The facts that the perforin-2 message level increased in BV2 cells and that HK or chloramphenicol-treated chlamydiae induced perforin-2 levels in HeLa cells suggest that alternative stimuli are capable of inducing perforin-2 expression. We speculate that microbial products liberated by the destruction of chlamydiae may be capable of stimulating through various pattern recognition receptors such as Toll-like receptors. In support of this notion, we have observed that addition of *Escherichia coli* lipopolysaccharide is able to stimulate perforin-2 expression in RAW267.4 cells (R. McCormack and E. R. Podack, unpublished data).

The observation that active chlamydial infection was able to interfere with perforin-2 and IDO protein levels was interesting. IFN-γ is essential for control of chlamydial infection *in vivo* (36), and IFN-γ is an agent capable of stimulating an aberrant or persistent growth state *in vitro* (37). Susceptibility of *C. trachomatis* to *in vitro* IFN-γ treatment is strain and cell type specific but is largely due to IDO-mediated catabolism of tryptophan (reviewed in reference 38). These results indicate that IDO is induced in the pres-

ence of IFN-γ, and this has been directly verified at the message and protein levels (39). Interestingly, these past studies required pretreatment of HeLa cells with IFN-γ. Our data indicate that an established *C. trachomatis* L2 infection is capable of inhibiting the expression of these two IFN-γ-responsive gene products. In agreement with the IDO protein levels, we did not detect any evidence of persistent chlamydial forms and there was no decrease in recovered progeny in cultures treated with IFN-γ (data not shown). *C. trachomatis* L2 is comparatively resistant to IFN-γ-mediated growth inhibition (40) and may possess mechanisms to inhibit specific antimicrobial factors. We did not test other chlamydial strains but predict that they are also capable of inhibiting IFN-γ-mediated induction of perforin-2. Pretreatment schemes used in other studies would induce perforin-2 prior to *Chlamydia* infection. However, the observation that chlamydial growth can be rescued by the addition of exogenous tryptophan (38) argues that perforin-2-mediated killing does not occur. Since our ectopic expression studies indicate that chlamydiae are susceptible to perforin-2, we conclude that either perforin-2 expression is blocked or chlamydial strains have additional defense mechanisms capable of resisting low levels of perforin-2 in epithelial cells. Additional work is required to discern which of these possibilities is correct.

There are multiple scenarios where perforin-2 could exert an impact on the *Chlamydia*-specific immune response. In the murine model, innate immunity is not sufficient for the resolution of chlamydial infections (reviewed in reference 10). However, it is clear that the innate response helps shape the course of infection. Infection of mice deficient in the signaling adapter MyD88 exhibit increased chlamydial burdens, increased times to resolution, and decreased recruitment of $CD4^+$ T cells (41). Mice deficient in effector mechanisms such as the production of nitric oxide clear genital infections normally (42–44) yet show altered susceptibility to infection-associated pathologies such as hydrosalpinx (45). Finally, monocytes and neutrophils infiltrate sites of chlamydial infection (9). Macrophages produce proinflammatory cytokines, and the degree of neutrophil influx correlates with the severity of hydrosalpinx (reviewed in reference 10). Therefore, perforin-2-expressing macrophages could play a direct role in the eradication of chlamydiae, thereby facilitating increases in macrophage-specific cytokine production. A role for perforin-2 during a successful adaptive response is also possible when epithelial cells are likely to be stimulated by IFN-γ or type I IFNs prior to infection. As the adaptive response matures, more uninfected epithelial cells would be induced to synthesize perforin-2 capable of limiting further cellular infection of mucosal surfaces. Therefore, perforin-2 may have a role in containing infections. Regardless of when perforin-2 contributes, our data predict that perforin-2 has a significant *in vivo* role in determining the outcome of the dynamic equilibrium that exists between the pathogen and the host defense.

The broad conservation of perforin-2 among eukaryotes, coupled with evidence that perforin-1 evolved from a duplication of *mpeg1* (46), is indicative of an primordial defense role for perforin-2. Likewise, coevolution of *Chlamydia* spp. with their eukaryotic hosts has an ancient history (47). Therefore, it makes sense that *Chlamydia* would need to contend with perforin-2 activity and in some cases evolve protective mechanisms to resist perforin-2-mediated killing. Perforin-2 is emerging as a central innate immune mechanism with a broad ability to neutralize intracellular bacteria. We have shown here that *C. trachomatis* is able to evade perforin-2 in cell types that represent favored replication niches, whereas perforin-2-mediated killing contributes significantly to the observed capacity of professional phagocytes to control chlamydial growth. These observations have important implications for understanding the overall immune response to chlamydial infection.

ACKNOWLEDGMENTS

We are grateful to Katerina Wolf, Greg Plano, Mathias Lichtenheld, and George Munson for fruitful conversations and critical reading of the manuscript. Electron microscopy was performed by M. Bates at the University of Miami Miller School of Medicine Electron Microscopy Core Facility. We thank Alison Quayle (Louisiana State University Health Science Center) for kindly providing A2EN cells and John Bethea (University of Miami) for BV2 cells.

K.A.F. was supported by a Public Health Service grant (AI065530) from the NIAID, National Institutes of Health. This work was supported by Public Health Service grants R01CA039201, P01 CA109094, R33AI0073234, and P01AI096396 to E.R.P. and F31AI106290 to R.M.

REFERENCES

1. **Morrison RP, Caldwell HD.** 2002. Immunity to murine chlamydial genital infection. Infect. Immun. **70:**2741–2751.
2. **Abdelrahman YM, Belland RJ.** 2005. The chlamydial developmental cycle. FEMS Microbiol. Rev. **29:**949–959.
3. **Hybiske K, Stephens RS.** 2007. Mechanisms of host cell exit by the intracellular bacterium *Chlamydia*. Proc. Natl. Acad. Sci. U. S. A. **104:**11430–11435.
4. **Moulder JW.** 1991. Interaction of chlamydiae and host cells in vitro. Microbiol. Rev. **55:**143–190.
5. **Fields KA, Hackstadt T.** 2002. The chlamydial inclusion: escape from the endocytic pathway. Annu. Rev. Cell Dev. Biol. **18:**221–245.
6. **Betts HJ, Wolf K, Fields KA.** 2009. Effector protein modulation of host cells: examples in the *Chlamydia* spp. arsenal. Curr. Opin. Microbiol. **12:**81–87.
7. **Valdivia RH.** 2008. *Chlamydia* effector proteins and new insights into chlamydial cellular microbiology. Curr. Opin. Microbiol. **11:**53–59.
8. **Fields KA.** 2012. Secretion mechanisms and *Chlamydia* pathogenesis, p 192–216. *In* Tan M, Bavoil P (ed), Intracellular pathogens. I. Chlamydiales. ASM Press, Washington, DC.
9. **Morrison SG, Morrison RP.** 2000. In situ analysis of the evolution of the primary immune response in murine *Chlamydia trachomatis* genital tract infection. Infect. Immun. **68:**2870–2879.
10. **Darville T, Hiltke TJ.** 2010. Pathogenesis of genital tract disease due to *Chlamydia trachomatis*. J. Infect. Dis. **201:**S114–S125.
11. **Beagley K, Huston W, PM H, Timms P.** 2009. Chlamydial infection of immune cells: altered function and implications for disease. Crit. Rev. Immunol. **29:**275–305.
12. **Sun HS, Eng EWY, Jeganathan S, Sin AT-W, Patel PC, Gracy E, Inman RD, Terebiznik MR, Harrision RE.** 2012. *Chlamydia trachomatis* vacuole maturation in infected macrophages. J. Leukoc. Biol. **92:**815–827.
13. **Yasir M, Pachikara ND, Bao X, Pan Z, Fan H.** 2011. Regulation of chlamydial infection by host autophagy and vacuolar ATPase-bearing organelles. Infect. Immun. **79:**4019–4028.
14. **Al-Zeer MA, Al-Younes HM, Lauster D, Abu Lubad M, Meyer TF.** 2013. Autophagy restricts *Chlamydia trachomatis* growth in human macrophages via IFNG-inducible guanylate binding proteins. Autophagy **9:**50–62.
15. **Spilsbury K, O'Mara M, Wu W, Rowe P, Symonds G, Takayama Y.** 1995. Isolation of a novel macrophage-specific gene by differential cDNA analysis. Blood **85:**1620–1629.
16. **Wiens M, Korzhev M, Krasko A, Thakur NL, Perović-Ottstadt S, Breter HJ, Ushijima H, Diehl-Seifert B, Muller IM, Muller WE.** 2005. Innate immune defense of the sponge Suberites domuncula against bacteria involves a MyD88-dependent signaling pathway. Induction of a perforin-like molecule. J. Biol. Chem. **280:**27949–27959.
17. **McCormack R, de Armas LR, Shiratsuchi M, Ramos JE, Podack ER.** 2013. Inhibition of intracellular bacterial replication in fibroblasts is dependent on the perforin-like protein (perforin-2) encoded by macrophage-expressed gene 1. J. Innate Immun. **5:**185–194.
18. **Wolf K, Fischer E, Hackstadt T.** 2005. Degradation of *Chlamydia pneu-*

moniae by peripheral blood monocytic cells. Infect. Immun. **73:**4560–4570.
19. **Caldwell HD, Kromhout J, Schachter J.** 1981. Purification and partial characterization of the major outer membrane protein of *Chlamydia trachomatis*. Infect. Immun. **31:**1161–1176.
20. **Furness G, Graham DM, Reeve P.** 1960. The titration of trachoma and inclusion blennorrhoea viruses in cell cultures. J. Gen. Microbiol. **23:**613–619.
21. **Laemmli UK.** 1970. Cleavage of structural proteins during the assembly of the head of bacteriophage T4. Nature **227:**680–685.
22. **Hackstadt T, Rockey DD, Heinzen RA, Scidmore MA.** 1996. *Chlamydia trachomatis* interrupts an exocytic pathway to acquire endogenously synthesized sphingomyelin in transit from the Golgi apparatus to the plasma membrane. EMBO J. **15:**964–977.
23. **Carabeo R, Grieshaber S, Fischer E, Hackstadt T.** 2002. *Chlamydia trachomatis* induces remodeling of the actin cytoskeleton during attachment and entry into HeLa cells. Infect. Immun. **70:**3793–3803.
24. **Scidmore-Carlson MA, Shaw EI, Dooley CA, Fischer ER, Hackstadt T.** 1999. Identification and characterization of a *Chlamydia trachomatis* early operon encoding four novel inclusion membrane proteins. Mol. Microbiol. **33:**753–765.
25. **Perry LL, Su H, Feilzer K, Messer R, Hughes S, Whitmire W, Caldwell HD.** 1999. Differential sensitivity of distinct *Chlamydia trachomatis* isolates to IFN-γ-mediated inhibition. J. Immunol. **162:**3541–3548.
26. **Chen AL, Johnson KA, Lee JK, Sütterlin C, Tan M.** 2012. CPAF: a chlamydial protease in search of an authentic substrate. PLoS Pathog. **8:**e1002842. doi:10.1371/journal.ppat.1002842.
27. **Lichtenheld MG, Olsen KJ, Lu P, Lowrey DM, Hameed A, Hengartner H, Podack ER.** 1988. Structure and function of human perforin. Nature **335:**448–451.
28. **DiScipio RG, Gehring MR, Podack ER, Kan CC, Hugli TE, Fey GH.** 1984. Nucleotide sequence of cDNA and derived amino acid sequence of human complement component C9. Proc. Natl. Acad. Sci. U. S. A. **81:**7298–7302.
29. **Podack ER, Tschopp J.** 1982. Polymerization of the ninth component of complement (C9): formation of poly(C9) with a tubular ultrastructure resembling the membrane attack complex of complement. Proc. Natl. Acad. Sci. U. S. A. **79:**574–578.
30. **Law RHP, Lukoyanova N, Voskoboinik I, Caradoc-Davies TT, Baran K, Dunstone MA, D'Angelo ME, Orlova EV, Coulibaly F, Verschoor S.** 2010. The structural basis for membrane binding and pore formation by lymphocyte perforin. Nature **468:**447–451.
31. **Baran K, Dunstone M, Chia J, Ciccone A, Browne KA, Clarke CP, Lukoyanova N, Saibil H, Whisstock JC, Vosoboinik I.** 2009. The molecular basis for perforin oligomerization and transmembrane pore assembly. Immunity **30:**684–695.
32. **Elwell CA, Engel JN.** 2012. Lipid acquisition by intracellular chlamydiae. Cell. Microbiol. **14:**1010–1018.
33. **Yong EC, Chi EY, Kuo CC.** 1987. Differential antimicrobial activity of human mononuclear phagocytes against the human biovars of *Chlamydia trachomatis*. J. Immunol. **139:**1297–1302.
34. **Wyrick PB, Brownridge EA, Ivins BE.** 1978. Interaction of *Chlamydia psittaci* with mouse peritoneal macrophages. Infect. Immun. **19:**1061–1067.
35. **Nagarajan UM, Ojcius DM, Stahl L, Rank RG, Darville T.** 2005. *Chlamydia trachomatis* induces expression of IFN-γ-inducible protein 10 and IFN-β independent of TLR2 and TLR4, but largely dependent on MyD88. J. Immunol. **175:**450–460.
36. **Rank RG, Whittum-Hudson JA.** 2010. Protective immunity to chlamydial genital infection: evidence from animal studies. J. Infect. Dis. **201:**S168–S177.
37. **Beatty WL, Morrison RP, Byrne GI.** 1994. Persistent chlamydiae: from cell culture to a paradigm for chlamydial pathogenesis. Microbiol. Rev. **58:**686–699.
38. **Wyrick PB.** 2010. *Chlamydia trachomatis* persistence in vitro: an overview. J. Infect. Dis. **201:**S88–S95.
39. **Roshick C, Wood H, Caldwell HD, McClarty G.** 2006. Comparison of gamma interferon-mediated antichlamydial defense mechanisms in human and mouse cells. Infect. Immun. **74:**225–238.
40. **Morrison RP.** 2000. Differential sensitivities of *Chlamydia trachomatis* strains to inhibitory effects of gamma interferon. Infect. Immun. **68:**6038–6040.
41. **Nagarajan UM, Sikes J, Prantner D, Andrews CW, Frazer L, Goodwin A, Snowden JN, Darville T.** 2011. MyD88 deficiency leads to decreased NK cell gamma interferon production and T cell recruitment during *Chlamydia muridarum* genital tract infection, but a predominant Th1 response and enhanced monocytic inflammation are associated with infection resolution. Infect. Immun. **79:**486–498.
42. **Igietseme JU, Perry LL, Ananaba GA, Uriri IM, Ojior OO, Kumar SN, Caldwell HD.** 1998. Chlamydial infection in inducible nitric oxide synthase knockout mice. Infect. Immun. **66:**1282–1286.
43. **Perry LL, Feilzer K, Caldwell HD.** 1998. Neither interleukin-6 nor inducible nitric oxide synthase is required for clearance of *Chlamydia trachomatis* from the murine genital tract epithelium. Infect. Immun. **66:**1265–1269.
44. **Ramsey KH, Miranpuri GS, Poulsen CE, Marthakis NB, Braune LM, Byrne GI.** 1998. Inducible nitric oxide synthase does not affect resolution of murine chlamydial genital tract infections or eradication of chlamydiae in primary murine cell culture. Infect. Immun. **66:**835–838.
45. **Ramsey KH.** 2001. Role for inducible nitric oxide synthase in protection from chronic *Chlamydia trachomatis* urogenital disease in mice and its regulation by oxygen free radicals. Infect. Immun. **69:**7374–7379.
46. **D'Angelo M, Dunstone M, Whisstock J, Trapani J, Bird P.** 2012. Perforin evolved from a gene duplication of MPEG1, followed by a complex pattern of gene gain and loss within *Euteleostomi*. BMC Evol. Biol. **12:**59. doi:10.1186/1471-2148-12-59.
47. **Clarke IN.** 2011. Evolution of *Chlamydia trachomatis*. Ann. N. Y. Acad. Sci. **1230:**E11–E18.